JAM CM Journal of Applied Mathematics and Computational Mechanics 2022, 21(4), 16-27
www.amcm.pcz.pl p-ISSN 2299-9965
DOI: 10.17512/jamcm.2022.4.02 e-ISSN 2353-0588

# SUDDENLY LOADED ARRAYS OF PILLARS WITH VARIABLE RANGE OF LOAD TRANSFER

***Tomasz Derda***

*Department of Mathematics, Czestochowa University of Technology*
*Czestochowa, Poland*
*tomasz.derda@pcz.pl*

Received: 23 September 2022; Accepted: 10 November 2022

**Abstract.** This paper deals with multicomponent systems subjected to suddenly applied loads. Such multicomponent systems consist of functionally identical elements, but the elements differ in their ability to sustain the applied load. Specifically, arrays of pillars are an example of the multicomponent systems. The capability of the array to sustain the applied load depends not only on the strength of the pillars but also on how the load coming from failed pillars is redistributed to the intact ones. We employ a Fiber Bundle Model with load transfer restricted within a rectangular region generated dynamically after each pillar's destruction. We investigate strength of the array and its survivability.

***MSC 2010:*** *82D30, 82D80, 65Z05*
***Keywords:*** *array of pillars, fiber bundle model, probability and statistics, strength, survivability*

## 1. Introduction

Progressing miniaturization is the current tendency that poses a challenge to understand the fracture size effects. Capturing how small-scale materials fail is a complex problem that has been extensively studied, as recently reviewed in [1]. Micro- and nanoscale materials are characterized by such remarkable properties as enhanced strength and toughness. However, these materials usually exhibit sample-to-sample fluctuations, and resulting size-effects are non-trivial.

An example of small scale devices is micro- and nanopillars assembled into arrays on the flat substrates [2]. Areas of applications of small-scale pillar arrays include e.g. bio-mechanical sensing, photovoltaics or nanoscale electronics. Multiple experimental studies on tensilely and compressively loaded metallic nanopillars approve the 'smaller is stronger' tenet i.e. a substantial strength increase is noticed with reduction of the sample size [3, 4]. The effect is observed in experiments performed on individual small-scale pillars. The present paper focuses on multicomponent systems composed of almost identical pillars that are subjected to axial sudden loading.

We apply the statistical approach implemented by the Fiber Bundle Model (FBM) concept [5,6]. In this scheme, the components whose strengths are smaller than loads locally imposed on them are immediately destroyed and carry no load. The load coming from failed components is transmitted to other intact elements according to a given load transfer rule. It is of crucial importance how such redistribution happens. Two extreme rules of load redistribution are global load sharing (GLS) and local load sharing (LLS). In the latter, only the nearest neighborhood is affected by the load originating from a failed component, and this rule is the most destructive one – the effective range of load transfer is very short. In this case, the local load concentration around a damage is very high, and cascades of broken components propagate to form an expanding cluster or clusters of failures. The GLS rule represents mean-field approximation where all the intact components in the system are equally affected by the load from a destroyed element irrespective of their distance from this element. In this scenario the effective range of interaction is infinite. Hence, damaged components may occur throughout the whole system. It is considered that the LLS rule simulates the behavior of the actual realistic materials more accurately [7].

The above-mentioned extreme rules are idealized ones. Hence, other rules are also proposed, e.g. power-law redistribution [8, 9] or transfer within the rectangular region generated by nearest intact neighbors in each direction [10, 11]. The effective range of load transfer can be tuned from global to (almost) local. In this work, we analyze the behavior of loaded pillar arrays by varying the range of the region including intact pillars. Specifically, we concentrate on maximum load supported by the arrays as well as their survivability under load.

The rest of the paper is organized as follows. In section 2, the applied model is described in detail. The simulation results are presented and discussed in section 3. The paper ends with a brief Conclusion section.

## 2. Model description

The considered system consists of $N = L \times L$ vertical pillars located on a flat substrate. The pillars are positioned in the nodes that form a square grid, therefore $L$ is the linear size of the system. Such pillar array is subjected to suddenly applied [9, 12, 13] axial load which induces pillar crushes. However, the pillars are functionally identical, but they differ in their quenched strength-thresholds $\sigma_{th}$. The differences in the pillar-strength thresholds are caused by inherent material defects or by fabrication errors. To take into account these pillar imperfections, we generate random pillar-strength-thresholds according to two-parameter Weibull distribution whose cumulative distribution function (cdf) is defined by

$$P_{\rho,\lambda}(\sigma_{th}) = 1 - \exp\left[-(\sigma_{th}/\lambda)^{\rho}\right]. \tag{1}$$

The shape parameter $\rho$ is responsible for the amount of disorder of thresholds. The parameter $\lambda$ scales a reference load. We assume here $\rho = 2$ and $\lambda = 1$.

In the analyzed loading scenario, the applied load rises suddenly from zero to a given value $F$. The initial increase of the load is uniform on all pillars in the system, hence the load applied per a single pillar is equal to $f = F/N$. The application of load $F$ causes failure of the pillars whose $\sigma_{th} < f$. Then, the load from the just destroyed pillars is redistributed to the pillars whose $\sigma_{th} \geq f$. The initial cascade of failures followed by load transfer may induce subsequent cascades of pillar failures and resulting load redistributions. At the end of the process the array achieves one of three stable states. The first possibility is the collapse of the array – all the pillars are destroyed. When the applied load $F$ is too small to destroy all the elements, the array freezes in a stable configuration with only a fraction of destroyed elements. The last scenario is the application of load that is too small to eliminate even the weakest pillars in the system. It is noted that during the whole process the load $F$ is conserved.

The load from a failed pillar is transferred uniformly to all intact pillars lying inside a rectangular region generated in the following way. We search intact pillars in four directions from the failed pillar until $R$ surviving ones are detected in each direction. The rectangular region is bounded from each side by the most distant surviving neighbor found in a given direction. An exemplary situation with $R = 1$ is depicted in Figure 1. The range of interaction is restricted to the shaded rectangular region. Intact pillars outside this region (and already destroyed elements) are not affected by load from the destroyed element. This is in contrast to the above-mentioned power law redistribution scheme where all the intact elements are affected, but the amount of load varies inversely with the distance from the destroyed element. In the analyzed model the effective range of load redistribution depends on which pillars are previously destroyed and which pillars are destroyed in the current time step (cascade). By varying the range of interaction $R$, we can pass from short range interactions to long range interactions.

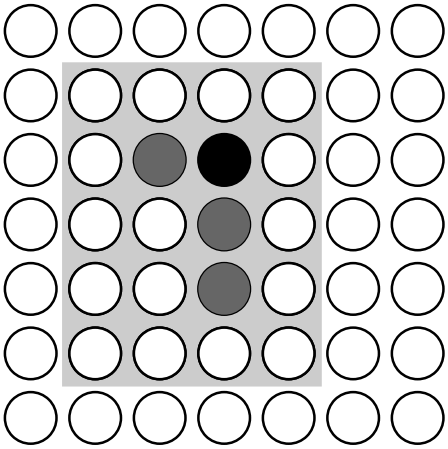

Fig. 1. The load transfer region for $R = 1$. Black circle denotes just broken pillar, whereas gray circles represent previously destroyed elements. The load redistribution from just destroyed pillar affects the intact pillars (denoted by empty circles) belonging to the shaded region

## 3. Simulation results

Based on the model described in the previous section, we have performed computer simulations of the loading processes of the pillar arrays. In our research, we applied Wolfram Mathematica software. During simulations, two quantities have been varied to observe different failure behaviors. The first quantity is the system size with $20 \times 20 \leq N \leq 160 \times 160$. This system size range is appropriate to examine the size effects in a reasonable computation time. The second varied quantity is the range $R$ with $1 \leq R < \sqrt{N}$.

Before the simulations of loading, we generated and stored at least $M = 5000$ uncorrelated sets $\{\sigma_{th}\}_N^{(j)}$, $j \in \{1,...,M\}$. Each set was drawn from Eq. (1). Then, taken one-by-one $\{\sigma_{th}\}_N^{(j)}$, we realized sudden compression experiments. However, these sudden loadings are carried out in two distinct ways, which correspond to two different purposes.

Our first goal is to obtain values of $f_{\max}^j(N,R)$, $j = 1,...,M$. We define $f_{\max}(N,R)$ as the maximum value of the initially applied load $f$ per pillar for which a particular array is in the precritical state [7]. This means that under $f_{\max}(N,R)$, the system supports the applied load, but even a small increase $\delta$ of the initial load induces system crossover to the postcritical state. In the precritical state the cascades of failures stop without breaking the entire system whereas in the postcritical state, all pillars in the system break.

Before simulation, we set a pair of values for $f_{\text{post}}$ and $f_{\text{pre}}$ corresponding to the postcritical and precritical states, respectively. The system is then loaded by the mean $f = \left(f_{\text{pre}} + f_{\text{post}}\right)/2$. If after the loading process the stable state is precritical the value of $f_{\text{pre}}$ is increased to $f$ otherwise $f_{\text{post}}$ is reduced to $f$. The simulation ends when the condition $f_{\text{post}} - f_{\text{pre}} \leq \min(0.0001, 1/N)$ is satisfied. We define the ultimate strength of the system $f_{\max}$ as the last recorded value of $f_{\text{pre}}$.

For a given system size and range $R$, simulation is repeated on $M$ independent configurations, and their strengths are averaged to obtain $\langle f_{\max}(N,R)\rangle$. Figure 2 illustrates chosen values of $\langle f_{\max}(N,R)\rangle$ in the function of $R$. In the regime of short range of interactions, $\langle f_{\max}\rangle$ rapidly increases as $R$ grows. Then, $\langle f_{\max}\rangle$ reaches a temporary plateau, after which a small increase is observed and $\langle f_{\max}\rangle$ achieves values corresponding to the GLS scheme.

In the case of the pure LLS scheme, a strong size effect of system strength is observed and $f_{\max}^{\text{LLS}} \to 0$ as $N \to \infty$. Similar behavior is observed for small values of $R$. However, this size effect weakens with increasing $R$ (Fig. 3). The adequate formula for fitting the LLS systems is given by

$$\langle f_{\max}^{\text{LLS}}(N)\rangle = \frac{\beta}{(\ln N)^{\alpha}} \tag{2}$$

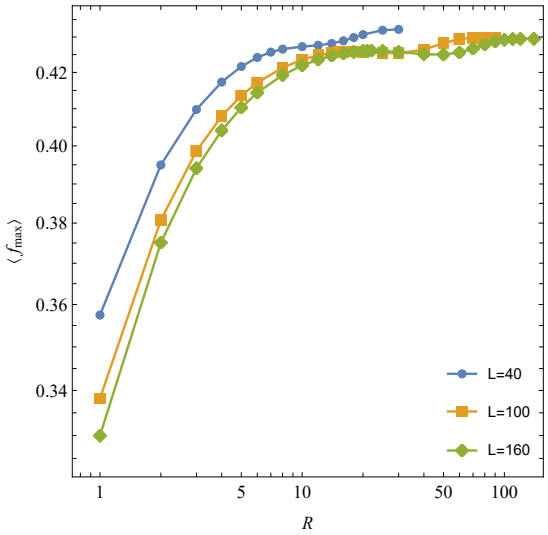


Fig. 2. Log-log plot of the mean strength of the system as a function of $R$. The solid lines are drawn to guide the eye

where $\beta = 0.631$ and $\alpha = 0.350$ (for $\rho = 2$). Considering model $R$, the formula (2) is adequate only for $R = 1$. However, even for $R = 1$, the size effect is weaker than it is for the pure LLS scheme. The effective range of interactions for $R = 1$ is substantially greater than it is for its LLS counterpart. The ratio $\langle f_{\max}(N,1)\rangle / \langle f_{\max}^{\mathrm{LLS}}(N)\rangle$ is an increasing function of $N$, taking 1.118 for $N = 20 \times 20$ and 1.177 for $N = 160 \times 160$. Hence, we propose the following formula with additional parameter

$$\langle f_{\max}(N,R)\rangle = \frac{\beta}{(\ln N)^{\alpha}} \left(1 + \eta N^{-\frac{2}{3}}\right). \tag{3}$$

This function can be used to approximate data up to $R = 8$. Exemplary fittings are graphically depicted in Figure 3. For $R/L \gtrapprox 0.5$, the array behaves like the pure GLS system with

$$0.995 < \frac{\langle f_{\max}(N,R)\rangle}{\langle f_{\max}^{\mathrm{GLS}}(N)\rangle} \leq 1. \tag{4}$$

The given array is able to sustain its $f_{\max}$, but under this suddenly applied load a considerable number of pillars is destroyed in the system. We define $U(N,R)$ as a fraction of surviving pillars under $f_{\max}$. Figure 4 graphically reports mean fractions of surviving pillars for chosen system sizes. Contrary to behavior of strength, the mean fraction $\langle U\rangle$ is a decreasing function of $R$. This means that in the systems with short range interactions the degree of destruction is (relatively) low, but the remaining intact fraction is able to support a relatively small load. A slight increase in the initially applied load $(f_{\max} + \delta)$ triggers self-sustained catastrophic avalanche of failures which also includes all the components that stay intact under $f_{\max}$. Systems

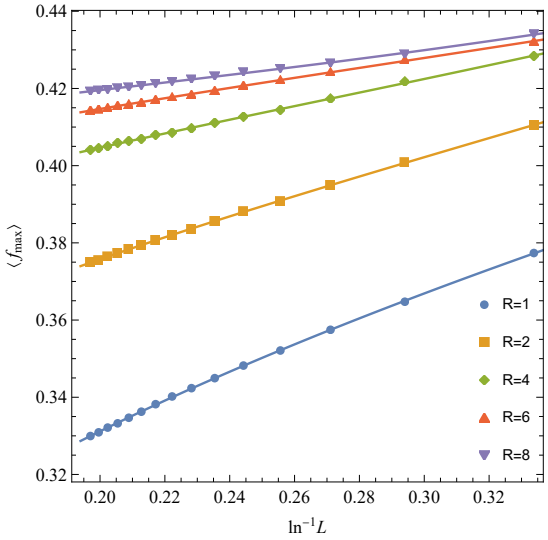


Fig. 3. The mean strength $\langle f_{\max} \rangle$ for arrays with $L \times L$ pillars. The solid lines are drawn according to formula (3)

with long range interactions are characterized by a relatively small fraction of surviving components which supports significantly higher load. This difference in behavior between short and long range regimes is caused by the degree of load transfer dispersion. In the short range regime the load is concentrated near broken components and, if the critical load $(f_{\max} + \delta)$ is applied, the destruction propagates through the system in the form of an expanding cluster (or clusters) of crushed pillars. In the case of long range interactions, significant load inhomogeneities are not present. All the intact pillars support similar load and thus the array sustains much higher load despite of the smaller fraction of surviving pillars.

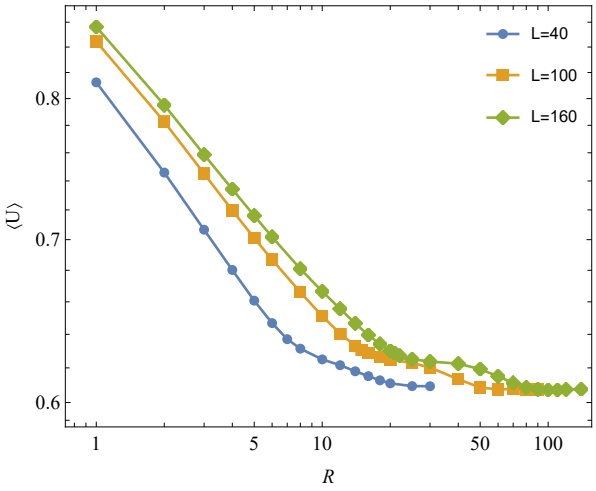


Fig. 4. Mean fraction of surviving pillars for systems loaded by their appropriate ultimate strengths

Ultimate strength of the system and fraction of broken pillars under $f_{\max}$ are random variables. We employ Pearson correlation coefficient $r$ to measure the strength of relationship between $f_{\max}$ and $U$. As $R$ grows, a gradual transition from highly negatively correlated data ($R = 1$) to almost uncorrelated data is observed (Fig. 5). The regime of long range interactions is characterized by negligibly small correlation. However, the behavior of $r$ as a function of $R$ is size dependent. Assuming short range interactions the bigger, the system the more correlated data are.

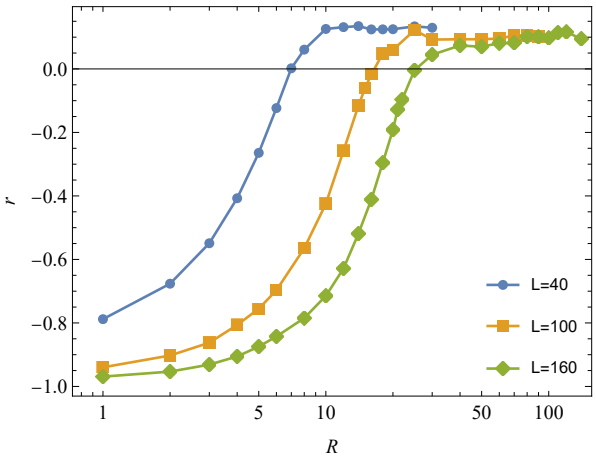


Fig. 5. Pearson correlation coefficient between $f_{\max}$ and $U$ as a function of range $R$

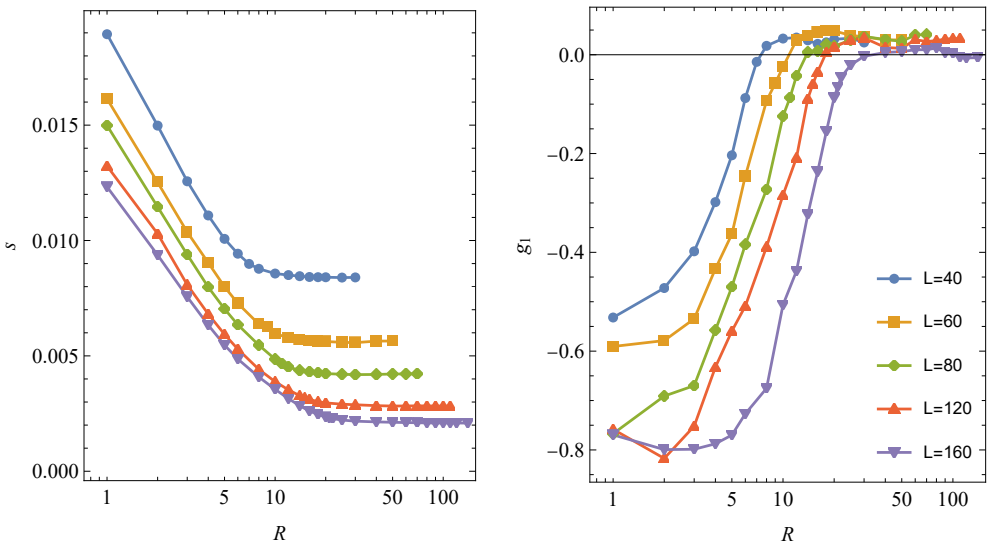


Fig. 6. Standard deviation ($s$, left panel) and skewness ($g_1$, right panel) of $f_{\max}$ distribution vs $R$

The above analyzed sample mean $\langle f_{\max} \rangle$ is an estimator of the mean of the population which is the first raw moment. We explore estimators of two other measures characterizing the distribution of $f_{\max}$, namely standard deviation $s$ (measure of dis-

persion of a distribution) and skewness $g_1$ (measure of the degree of asymmetry). These two measures are calculated from central moments. The results are shown in Figure 6. From the left panel it is seen that the dispersion of $f_{\max}$ decreases as the range of interactions grows. From a certain value of $R$, dependent of system size, the standard deviation becomes almost constant. In this range of $R$ the arrays present the GLS-like behavior.

Regarding the skewness (right panel of Fig. 6), the distribution of $f_{\max}$ changes from moderately skewed to non-skewed as the entire range of $R$ is passed. Some fluctuations, visible in the right panel of Figure 6, are caused by too small a sample size $M$ as the skewness is computed from the third central moment. However, the trend is clear. The skewness vanishes ($|g_1| < 0.1$) at approximately $R/L \in (0.12, 0.16)$.

As the distribution of $f_{\max}$ varies from moderately skewed to symmetrical, we employ three-parameter skew normal distribution (SND) for fitting $f_{\max}$ distribution. The SND is a generalization of the Gaussian distribution that allows non-zero skewness. The cumulative distribution function (cdf) of SND follows

$$P(f_{\max}) = \frac{1}{2}\operatorname{erfc}\left(-\frac{f_{\max}-\xi}{\sqrt{2}\omega}\right) - 2\mathrm{T}\left(\frac{f_{\max}-\xi}{\omega}, \zeta\right) \tag{5}$$

where $\mathrm{T}(\cdot,\cdot)$ is Owen's T function and $\xi$, $\omega$, $\zeta$ represent location, scale and shape parameters, respectively. The last parameter governs the skewness. The empirical parameters have been determined by the maximum likelihood method. Exemplary empirical probability density (pdf) functions are presented in Figure 7. Goodness-of--fit has been tested using Cramér-von Mises and Anderson-Darling methods.

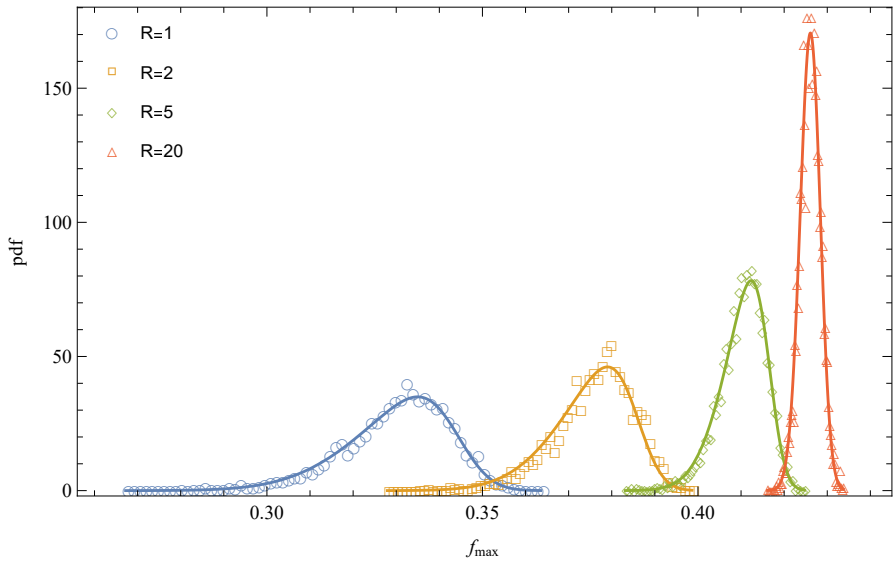


Fig. 7. Empirical probability density functions for different values of $R$ and $N = 160 \times 160$. Solid lines are drawn according to Eq. (5) with parameters approximated to fit the empirical data

As the skewness decreases and finally vanishes with increasing $R$, we have conducted Shapiro-Wilk tests for normality testing of $f_{\max}$ distribution. This allowed us to evaluate the minimum values of $R$ from which the data follow normal distribution (characteristic for the GLS regime). These minimum values are shown in Figure 8. A clear size effect is visible. For values of $R$ smaller than reported in Figure 8, the Shapiro-Wilk tests return $p$-value $< 0.05$ showing evidence that in this range of $R$ the data are not normally distributed. Hence, the data is skewed, which is typical for the LLS rule and short range interactions. Therefore, values of $R$ presented in Figure 8 may indicate transition points between two regimes, namely short and long range interactions.

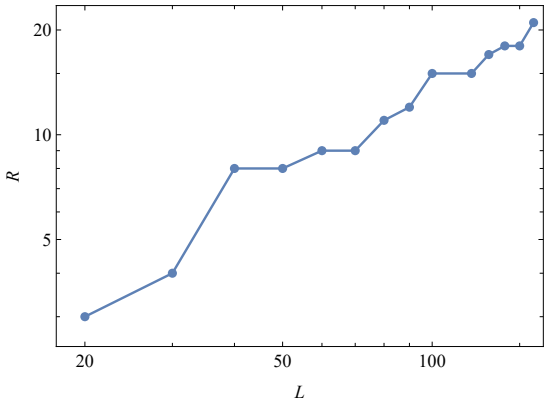


Fig. 8. The minimum values of $R$ for which Shapiro-Wilk tests have $p$-value $> 0.05$. Normality of $f_{\max}$ distribution is tested

The second goal of the paper is analysis of array survivability. Survival of the array means that, after the loading procedure, the array sustains the applied load, meaning that the precritical stable state is reached. Let survival function $S(f)$ be a measure of survivability. We define the survival function $S(f)$ as the probability that a given array is in the precritical state when the load $f$ (or less) is applied to the system. The survival function can be viewed as the fraction of arrays having survived until load $f$.

For a fixed system size, we have chosen a suitable range of $f$ to ensure covering the range from $S(f) \approx 1$ to $S(f) \approx 0$ for each analyzed $R$. Then, taking each set $\{\sigma_{th}\}$, we have performed loading processes for increasing values of $f$ at a step of $\Delta f = 0.001$.

The survival curves are fitted by the complementary cdfs of skew normal distribution

$$S(f) = 1 - \frac{1}{2}\mathrm{erfc}\left(-\frac{f-\xi_{SF}}{\sqrt{2}\omega_{SF}}\right) + 2\mathrm{T}\left(\frac{f-\xi_{SF}}{\omega_{SF}}, \zeta_{SF}\right) \tag{6}$$

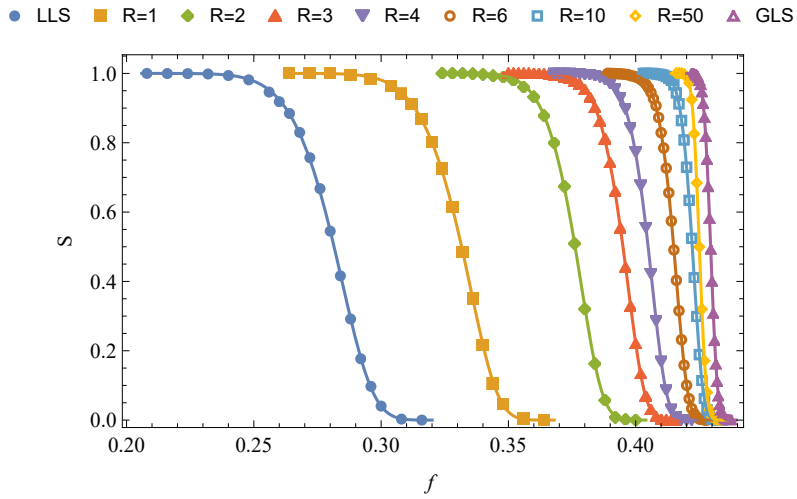


Fig. 9. Empirical survival functions for different values of $R$. The cases of LLS and GLS rule are also included. System size $N = 160 \times 160$. Solid lines follow Eq. (6) with parameters computed from the simulations

where $\xi_{SF}$, $\omega_{SF}$, $\zeta_{SF}$ are parameters that correspond to location, scale and shape, respectively. Exemplary fittings, together with data points obtained from simulations, are drawn in Figure 9. Results concerning the LLS and the GLS schemes are also attached. A considerable shift to the right of the survival curve is observed when the range of interactions changes from pure LLS to $R = 1$. As $R$ increases, the transition region from $S(f) \approx 1$ to $S(f) \approx 0$ decreases. Values of fitted parameters $\xi_{SF}$, $\omega_{SF}$, $\zeta_{SF}$ are presented in Figure 10. The previously mentioned system size effect is also seen in the results concerning survival curves. Values of all parameters are arranged in a descending order of the system size. The behavior of $\xi_{SF}$, $\omega_{SF}$ and $\zeta_{SF}$ parameters is similar to the one observed for $\langle f_{\max} \rangle$, $s$ and $g_1$, respectively. Furthermore, values of the expectation

$$\mu = \int_0^\infty S(f) \mathrm{d}f. \tag{7}$$

are perfectly consistent with values of $\langle f_{\max} \rangle$, however, these two measures are obtained from two different processes.

## 4. Conclusions

We have numerically simulated axial sudden loadings of pillar arrays. The strength--thresholds of the pillars were quenched random variables distributed according to Weibull distribution.

After the destruction of the pillar, its load has to be transferred to other intact pillars. Hence, load transfer rule plays a key role in the loading process. We have

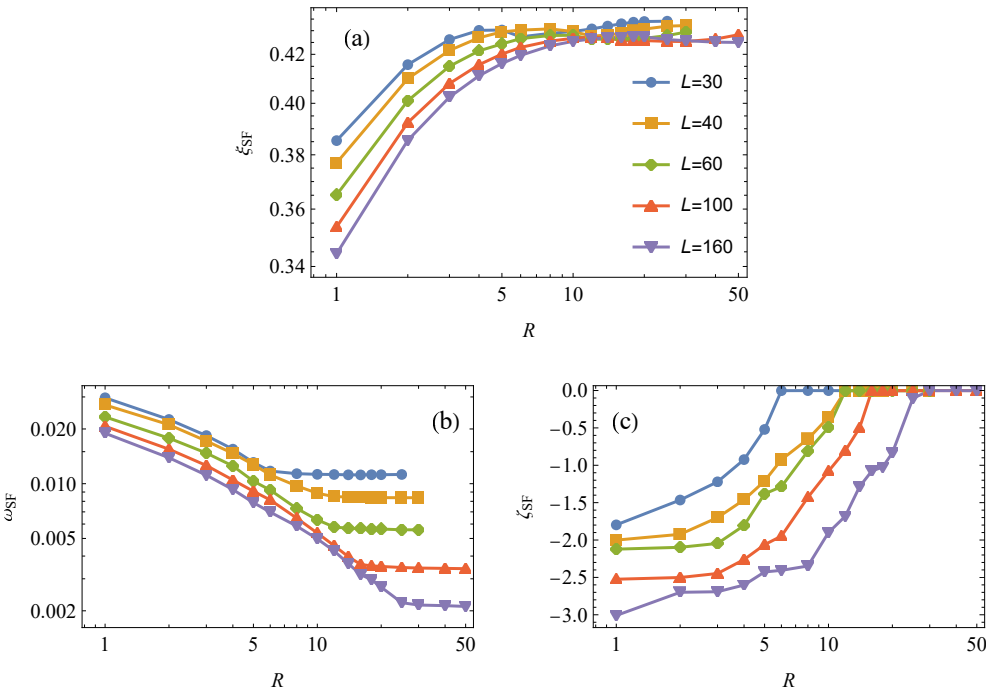


Fig. 10. The approximated parameters $\xi_{SF}$ (a), $\omega_{SF}$ (b) and $\zeta_{SF}$ (c) vs. $R$ for chosen system sizes

employed uniform load transfer within rectangular array of range $R$. The parameter $R$ allows us to tune the effective range of interactions from short (LLS-like) to long range (GLS-like).

Obtained values of maximum load $f_{\max}$ turned out to be a function of system size $N$ and range of interaction $R$. Based on the simulation results, we have shown that the empirical distribution of $f_{\max}$ follows skew normal distribution. However, the skewness vanishes as the system crosses from short to long range interactions.

For the fixed value of $R$, we have found the formula for the mean system strength in the function of the system size. The formula is adequate up to $R = 8$. Considering array survivability, we have fitted survival curves by complementary cumulative of skew normal distribution. Values of fitted parameters are arranged according to the system size.

## References

[1] Taloni, A., Vodret, M., Costantini G., & Zapperi S. (2018). Size effects on the fracture of microscale and nanoscale materials. *Nature Reviews Materials*, *3*, 211-224.

[2] Park, J.E., Won, S., Cho, W., Kim, J.G., Jhang, S., Lee, J.G., & Wie, J.J. (2021). Fabrication and applications of stimuli-responsive micro/nanopillar arrays. *Journal of Polymer Science*, *59*, 1491.

[3] Jang, D., & Greer, J.R. (2010). Transition from a strong-yet-brittle to a stronger-and-ductile state by size reduction of metallic glasses. *Nature Materials*, *9*, 215-219.

[4] Uchic, M.D., Dimiduk, D.M., Florando, J.N., & Nix, W.D. (2004). Sample dimensions influence strength and crystal plasticity. *Science*, *305*, 986-989.

[5] Hansen, A., Hemmer, P.C., & Pradhan, S. (2015). *The Fiber Bundle Model: Modeling Failure in Materials*. Wiley-VCH.

[6] Derda, T. (2017). Statistical analysis of mechanical damage in nanopillar arrays with mixed--mode load transfer. *Journal of Applied Mathematics and Computational Mechanics*, *6*(3), 5-16.

[7] Roy, Ch., Kundu, S., & Manna, S.S. (2013). Scaling forms for relaxation times of the fiber bundle model. *Physical Review E*, *87*, 062137.

[8] Hidalgo, R.C., Moreno, Y., Kun, F., & Herrmann, H.J. (2002). Fracture model with variable range of interaction. *Physical Review E*, *65*, 046148.

[9] Biswas, S., & Goehring, L. (2016). Interface propagation in fiber bundles: local, mean-field and intermediate range-dependent statistics. *New Journal of Physycs*, *18*, 103048.

[10] Roy, S., Biswas, S., & Ray, P. (2017). Modes of failure in disordered solids. *Physical Review E*, *96*, 063003.

[11] Roy, S., Biswas, S., & Ray, P. (2019). Failure time in heterogeneous systems. *Physical Review Research*, *1*, 033047.

[12] Biswas, S., & Sen, P. (2015). Maximizing the strength of fiber bundles under uniform loading. *Physical Review Letters*, *115*, 155501.

[13] Derda, T., & Domanski Z., (2021). Survivability of suddenly loaded arrays of micropillars. *Materials*, *14*(23), 7173.